Photorefractive-gain dependence on piezoelectric and photoelastic effects in barium titanate

Pierre Mathey*
Matériaux pour l'Optique Non-Linéaire, Laboratoire de Physique de l'Université de Bourgogne, UPRES-A CNRS 5027, 9 Avenue Alain Savary, Boîte Postale 400, 21011 Dijon Cedex, France
(Received 25 November 1996)

The influence of the piezoelectric and photoelastic effects is experimentally demonstrated in barium titanate ($BaTiO_3$). Its effect on the photorefractive two-beam coupling is investigated for extraordinary and ordinary polarizations. Two additional maxima in the photorefractive extraordinary gain are found and correspond to the two sidelobes of beam fanning. The role of the trap density on their magnitude and angular position is theoretically studied. [S1063-651X(97)07906-3]

PACS number(s): 42.70.Nq, 42.65.Hw, 77.84.Dy, 78.20.Hp

The large value of the electro-optic coefficient r_{42} makes barium titanate ($BaTiO_3$) an interesting material for optical nonlinear applications where photorefractive effects occur [1]: image amplification, novelty filtering, optical correlation, wave-front correction via phase conjugation, and holography. The physics of the photorefractive effect is now well understood. Two coherent beams interfere inside the material. A photorefractive grating results from a photoinduced charge redistribution in the bulk of the material. The associated photoinduced electric field, in turn, generates an index change. Each beam is self-diffracted by the index grating and adds constructively or destructively with the incident beam. The consequence is that the intensity of one beam is decreased while the intensity of the other beam is amplified. Most of the applications involve two waves mixing and imply energy transfer from a pump beam to a weak beam (the probe or the signal beam). The efficiency of the energy transfer is characterized by the two-beam coupling gain Γ expressed as [1]:

$$\Gamma = \vartheta(I)\,\frac{2\pi}{\lambda}\,(n_p n_s)^{3/2} r_{\mathrm{eff}} E_{\mathrm{sc}} \langle \vec{e}_p \cdot \vec{e}_s \rangle, \tag{1}$$

where $\vartheta(I)$ is a saturation parameter that depends on the intensities and increases up to a value of 1 [2], λ is the wavelength of light in vacuum, n_p and n_s are the refractive indices of the pump and the signal waves, respectively, $\vec{e}_p$ and $\vec{e}_s$ are unitary polarization vectors of the beams, r_{eff} is the effective electro-optic coefficient, and E_{sc} is the space-charge electric field whose expression is, in absence of an external electric field and in the presence of one deep and one shallow site:

$$E_{\mathrm{sc}} = \frac{E_d E_q}{E_d + E_q} \tag{2}$$

with

$$E_d = \frac{k_B T K}{e} \tag{3}$$

$$E_q = \frac{e N_A}{\epsilon_0 \epsilon_{\mathrm{eff}} K} \tag{4}$$

where e is the electron charge, k_B is the Boltzmann's constant, T is the temperature, ϵ_0 is the vacuum permittivity, K is the grating vector modulus, and N_A is the trap density. In the above formulations, two important quantities appear: the photorefractive effective dielectric constant ϵ_{eff} [see Eq. (4)] and the effective electro-optic coefficient [see Eq. (1)]. In the ten last years, there has been controversy about their expressions, especially in determining which of the clamped (strain free) or unclamped (stress free) coefficients should be used in materials where a constant electric field is applied [3,4]. Moreover, it has been demonstrated that in materials where spatially modulated electric fields occur, as it is the case in a two-waves mixing configuration, the effective dielectric and electro-optic coefficients are neither the clamped nor the unclamped coefficients, but they can be calculated from these values [5,6]. Günter and Zgonik [7] consider each kind of deformation and give the two appropriate coefficients as combinations of piezoelectric and photoelastic tensor components:

$$\epsilon_{\mathrm{eff}} = g_i g_j \epsilon_{ij}^S + \frac{e_{ijk} e_{mnl} g_i g_j g_m g_n A_{kl}^{-1}}{\epsilon_0}, \tag{5}$$

$$r_{\mathrm{eff}} = d_{p,i} d_{s,j} [r_{ijk}^S g_k + p'^E_{ijkl} g_l A_{km}^{-1} B_m]. \tag{6}$$

g_i, g_j, g_m, g_n, and g_k are components of the unitary grating vector $\vec{g} = \vec{K}/K$, ϵ_{ij}^S is the static clamped dielectric tensor, ϵ_0 is the vacuum permeability, e_{ijk} is the piezoelectric stress tensor, r_{ijk}^S is the clamped electro-optic tensor, $d_{p,i}$, $d_{s,j}$ are components of unit vectors along the dielectric displacement vectors, $B_m = e_{kmj} g_k g_j$, $A_{ik} = C_{ijkl}^E g_j g_l$, C_{ijkl}^E is the elastic stiffness tensor, and $p'^E_{ijkl} = p^E_{ij(kl)} + p^E_{ij[kl]}$ is the elasto-optic tensor at a constant field that takes into account the Pockels effect $p^E_{ij(kl)}$ and the rotation of the index ellipsoid [8,9] via

$$p^E_{ij[kl]} = -p^E_{ij[lk]} = \frac{1}{2}\left[\left(\frac{1}{n^2}\right)_{ii} - \left(\frac{1}{n^2}\right)_{jj}\right](\delta_{il}\delta_{jk} - \delta_{ik}\delta_{jl}). \tag{7}$$

*Electronic address: pmathey@u-bourgogne.fr

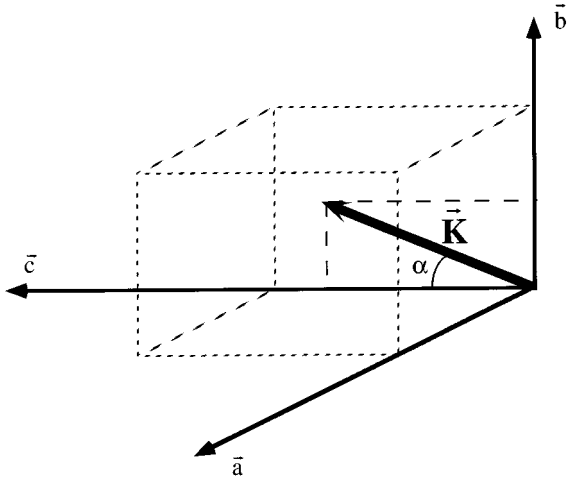

FIG. 1. Scheme of the crystallographic axis and grating vector $\vec{K}$ that results from the interference of the pump beam and the probe beam. The crystal is rotated around its $\vec{a}$ axis, the grating vector $\vec{K}$ stays in the plane $(\vec{b},\vec{c})$.

The above theoretical development successfully explains the beam fanning structure in $BaTiO_3$ [10] that appears when extraordinary light passes through this material. The beam fanning phenomenon arises from the selective amplification of light scattered from various defects in the bulk and surface irregularities through beam coupling with the incident beam itself. The far-field resulting intensity results in a three-lobed structure composed by a central lobe along the $\vec{c}$ axis and two side lobes apart from the central lobe. In the previous work [10], the beam was supposed to be scattered (and thus diverging) according to a Gaussian law with half-width of 24°. In the present study, we present proofs of the expressions (5) and (6) with two-beam coupling experiments involving single plane waves that do not diverge or converge inside the crystal. In our experimental setup, the pump and probe beams impinge onto the crystal at symmetric angles $\theta=20°$ measured in the air, writing a grating whose vector is perpendicular to the $\vec{a}$ axis. The normal to the entrance face of the crystal is $\vec{a}$ (see Fig. 1). The undoped $BaTiO_3$ sample is rotated around its $\vec{a}$ axis by an angle $\alpha=(\vec{K},\vec{c})$, the $\vec{K}$ vector staying in the $(\vec{b},\vec{c})$ plane. For several α values, the steady-state photorefractive gain Γ is measured, the polarization of the waves being adjusted for each angle α with half wave plates to keep them both ordinary if ordinary gain is experienced or extraordinary in the case of extraordinary gain. The results conducted at $\lambda=633$ nm with a pump-probe ratio 3×10^4 are depicted in Fig. 2(a) for extraordinary waves and in Fig. 2(b) for ordinary waves. Two secondary maxima at $\alpha\approx\pm50°$ apart from the central maximum are found, these positions do agree with the two sidelobe directions of the beam fanning observed in this crystal at this wavelength. In each case, the curve in the solid line is the theoretical gain Γ calculated with Eq. (1). All the numerical data concerning the dielectric constants, the piezoelectric, elasto-optic, and electro-optic coefficients are extracted from [11]. The trap density for this crystal is $N_A=3\times10^{22}$ m^{-3} determined from classical gain measurements versus θ at the same wavelength. The incident light intensity being $I=10$ mW/cm^2 is well below the saturation intensity so that the parameter $\vartheta(I)$ can take a value different from unity: it is taken equal to 0.55 for every theoretical curve in Fig. 2(a) and 2(b). The dashed curves are obtained if the piezoelectric and photoelastic effects are neglected and if only unclamped coefficients [11] are intended instead of the clamped ones. In this case, the effective coefficients take the form:

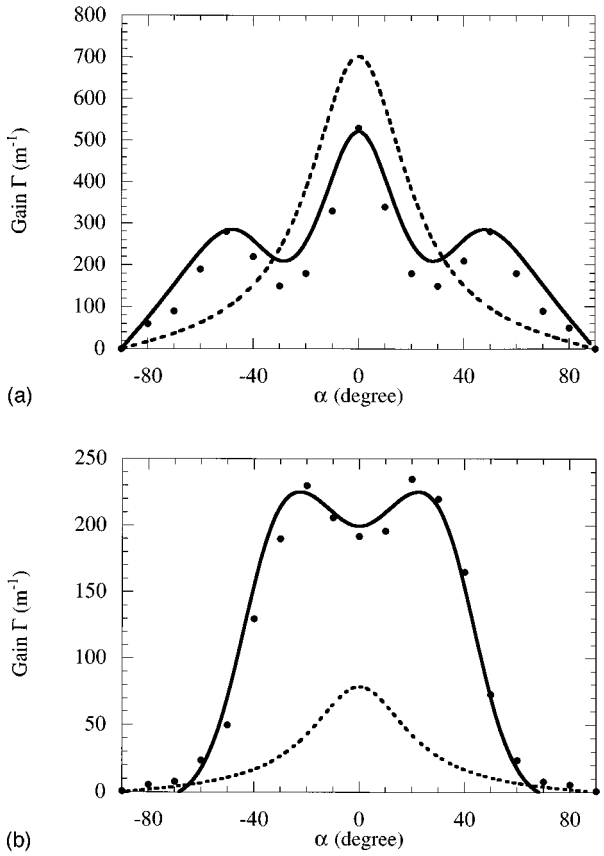

FIG. 2. Photorefractive extraordinary [Fig. 2(a)] and ordinary [Fig. 2(b)] gain Γ versus the angle α at $\lambda=633$ nm, in a pure $BaTiO_3$ crystal. The experimental results are represented by dots. The curves in full lines correspond to the theoretical expressions (1), (5), and (6). The curves in dashed lines are obtained by neglecting the piezoelectric and photoelastic contributions.

$$\epsilon_{\text{eff}}=g_i g_j \epsilon_{ij}^T, \tag{8}$$

$$r_{\text{eff}}=d_{p,i}d_{p,j}r_{ijk}^T g_k. \tag{9}$$

Similar measurements conducted at $\lambda=514$ nm with the same crystal and with a pump-probe ratio of 2×10^3 lead to the same conclusions. Two additional regions at $\alpha\approx\pm50°$ with high amplification are again detected. Further experiments with a pump beam and a probe beam asymmetrically incident with respect to the $\vec{a}$ axis give higher gains (due to the coefficient r_{42}) and confirm the existence of the side maxima at the same positions as above.

In summary, two regions outside the classical one are found in the gain curves and explained with the influence of the piezoelectric and photoelastic effects, this for ordinary

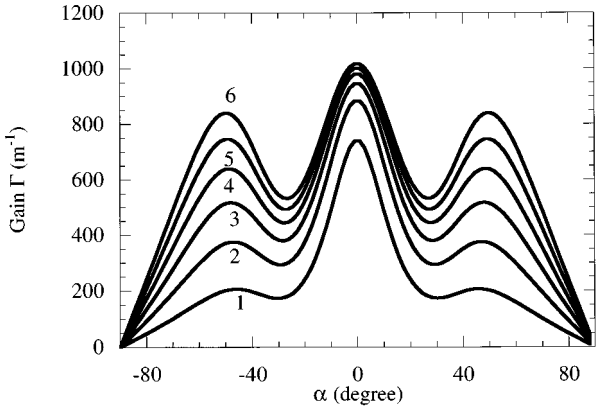

FIG. 3. Theoretical gain Γ versus the angle α at $\lambda = 633$ nm in a pure $BaTiO_3$ crystal, for several trap densities in the range [1 $\times 10^{22}$ m^{-3}; 6$\times 10^{22}$ m^{-3}] (curve 1 to curve 6).

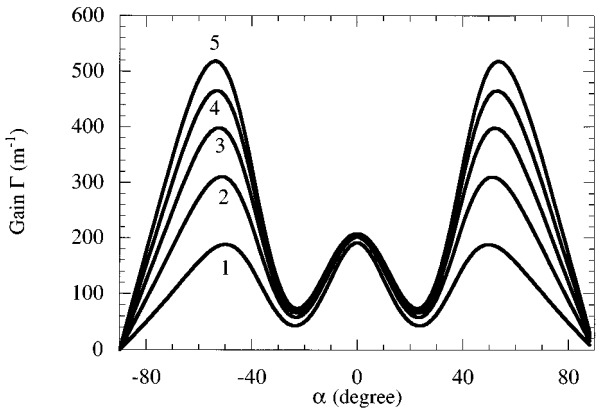

FIG. 4. Theoretical gain Γ versus the angle α at $\lambda = 1064$ nm in a Rh:$BaTiO_3$ crystal, for several trap densities in the range [1 $\times 10^{22}$ m^{-3}; 5$\times 10^{22}$ m^{-3}] (curve 1 to curve 5).

polarized waves as well as for extraordinary polarized waves. The role of the trap density N_A is illustrated in Fig. 3. As this quantity is increased, the maximum gain obtained for $\alpha = 0°$ takes greater values, and reaches a saturation value of $\Gamma_s \approx 10$ cm^{-1} for $N_A > 4\times 10^{22}$ m^{-3}. This parameter slightly alters the angular positions of the secondary maxima; its major effect is to increase their magnitude that becomes closer and closer to the central gain value Γ_s. Such samples should be very efficient when the depletion of one bearing beam is researched as in novelty filter arrangements.

To go further with predictions, it is interesting to investigate the same effect in rhodium doped $BaTiO_3$. It has been recently discovered [12–14] that these crystals perform well in the near infrared region, opening fruitful perspectives for the applications at the laser diode wavelength. The evolution of the theoretical gain versus the angle α is drawn in Fig. 4, at $\lambda = 1.064$ μm. The values of the tensorial coefficients are issued from Refs. [15, 16]. At this wavelength, the two side maxima are positioned at $\alpha \approx \pm 50°$. A particular effect is the strong increasing of the side maxima magnitude for relative small N_A values.

In conclusion, the influence of the piezoelectric and photoelastic effects has been experimentally depicted with photorefractive two-beam coupling arrangements. The existence of two side regions where the gain is privileged is confirmed. The interpretation of the results does not need the hypothesis of a scattered beam according to a Gaussian law whose half-width value is not easy to verify. It has also been shown that the location of the side maxima is independent of the trap density. This last quantity acts on their magnitude, allowing greater energy transfer in the side lobes than in the central one for Rh:$BaTiO_3$.

ACKNOWLEDGMENTS

The author thanks Doctor P. Jullien for his useful comments on the manuscript and helpful discussions.

[1] *Photorefractive Materials and Their Applications* I, edited by P. Günter and J. P. Huignard, Topics in Applied Physics, Vol. 62 (Springer-Verlag, Berlin, 1989).
[2] P. Tayebati and D. Mahgerefteh, J. Opt. Soc. Am. **8**, 1053 (1991).
[3] S. I. Stepanov, S. M. Shandarov, and N. D. Khatkov, Sov. Phys. Solid State **29**, 1754 (1987).
[4] A. Schaeffer, H. Schmitt, and A. Dörr, Ferroelectrics **69**, 253 (1986).
[5] G. Pauliat, P. Mathey, and G. Roosen, J. Opt. Soc. Am. **8**, 1942 (1991).
[6] S. Shandarov, Appl. Phys. A **55**, 91 (1992).
[7] P. Günter and M. Zgonik, Opt. Lett. **16**, 1826 (1991).
[8] D. F. Nelson and M. Lax, Phys. Rev. Lett. **24**, 379 (1970).
[9] D. F. Nelson and P. D. Lazay, Phys. Rev. Lett. **25**, 1187 (1970).
[10] G. Montemezzani, A. A. Zozulya, L. Czaia, D. Z. Anderson, M. Zgonik, and P. Günter, Phys. Rev. A **52**, 1791 (1995).
[11] M. Zgonik, P. Bernasconi, M. Duelli, R. Schlesser, P. Günter, M. H. Garrett, D. Rytz, Y. Zhu, and X. Wu, Phys. Rev. B **50**, 5941 (1994).
[12] M. Kaczmarek, G. W. Ross, P. M. Jeffrey, R. W. Eason, P. Hribek, M. J. Damzen, R. Ramos-Garcia, R. Troth, M. H. Garrett, and D. Rytz, Opt. Mater. **4**, 158 (1995).
[13] H. Kröse, R. Scharfschwerdt, O. F. Schirmer, and H. Hesse, Appl. Phys. B **61**, 1 (1995).
[14] M. Kaczmarek and R. W. Eason, Opt. Lett. **20**, 1850 (1995).
[15] K. Buse, S. Rihemann, S. Loheide, H. Hesse, F. Mersch, and E. Krätzig, Phys. Status Solidi A **K87**, 135 (1993).
[16] P. Bernasconi, M. Zgonik, and P. Günter, J. Appl. Phys. **78**, 2651 (1995).